

Article citation info:

Nycz D B. Influence of selected design parameters of the composite-foam cover rail on the course of the TB11 crash test of a road safety barrier forming a horizontal concave arc. The Archives of Automotive Engineering – Archiwum Motoryzacji. 2017; 76(2) 107-122: <http://dx.doi.org/10.14669/AM.VOL76.ART5>

INFLUENCE OF SELECTED DESIGN PARAMETERS OF THE COMPOSITE-FOAM COVER RAIL ON THE COURSE OF THE TB11 CRASH TEST OF A ROAD SAFETY BARRIER FORMING A HORIZONTAL CONCAVE ARC

WPŁYW WYBRANYCH PARAMETRÓW KONSTRUKCYJNYCH NAKŁADKI KOMPOZYTOWO-PIANOWEJ NA PRZEBIEG TESTU ZDERZENIOWEGO TB11 DROGOWEJ BARIERY OCHRONNEJ W ŁUKU POZIOMYM WKŁĘŚŁYM

DANIEL B. NYCZ¹

Jan Grodek State Vocational Academy in Sanok

Summary

The article presents a numerical examination of the influence of selected design parameters of a CFR2 composite-foam cover rail of a roadside barrier (described in previous publications by the same author) on the course of the TB11 virtual crash test. The crash tests were carried out on a modified SP-05/2

¹ Jan Grodek State Vocational Academy in Sanok, Technical Institute, ul. Reymonta 6, 38-500 Sanok, Poland:
e-mail: e-mail: daniel.nycz@interia.pl

barrier of the N2-W4-A class, forming a horizontal concave arc with a radius of 150 m. During the tests, a passenger car with a mass of 900 kg hit the barrier with a velocity of 100 km/h at an angle of 20°. The CFR2 cover rail consists of polyester-glass composite segments partly filled with polyurethane foam. The cover rail cross-section fits the B-type guiderail profile of the barrier. The numerical computations were carried out in the LS-Dyna environment, with using the Geo Metro vehicle model taken from the NCAC website and subjected to necessary modifications. The results of the virtual crash tests were analysed in respect of all the qualitative and quantitative parameters required by standards PN-EN 1317-1:2010 and PN-EN 1317-2:2010. The analyses carried out showed the design of the CFR2 cover rail to be correct and sufficient for the TB11 crash test results to be accepted.

Keywords: TB11 virtual crash test, barrier forming a horizontal concave arc, composite-foam cover rail, cover rail design parameters

Streszczenie

W pracy przedstawiono badania numeryczne wpływu wybranych parametrów konstrukcyjnych nakładki kompozytowo-pianowej CFR2 (opisanej w poprzednich publikacjach autora) na przebieg wirtualnego testu zderzeniowego TB11. Testy zderzeniowe obejmują zmodyfikowaną barierę SP-05/2 klasy N2-W4-A, tj. w łuku poziomym wklęsłym o promieniu 150 m. Test TB11 dotyczy samochodu osobowego o masie 900 kg, uderzającego w barierę z prędkością 100 km/h pod kątem 20°. Nakładka CFR2 składa się z segmentów kompozytowych poliestrowo-szklanych, częściowo wypełnionych pianką poliuretanową. Przekrój poprzeczny nakładki jest dopasowany do prowadnicy typu B. Obliczenia numeryczne przeprowadzono w środowisku LS-Dyna z wykorzystaniem modelu pojazdu Geo Metro, pobranego ze strony NCAC i poddanego niezbędnym modyfikacjom. Wyniki wirtualnych testów zderzeniowych przeanalizowano pod kątem wszystkich parametrów jakościowych i ilościowych wymaganych przez normy PN-EN 1317-1:2010 i PN-EN 1317-2:2010. Przeprowadzone analizy wykazały, że konstrukcja nakładki CFR2 jest trafna i wystarczająca do zapewnienia przyjęcia badania zderzeniowego TB11.

Słowa kluczowe: wirtualny test zderzeniowy TB11, bariera w łuku poziomym wklęsłym, nakładka kompozytowo-pianowa, parametry konstrukcyjne nakładki

1. Introduction

There are many publications dedicated to virtual crash tests and such tests are used to examine various road restraint systems, including steel [1, 6, 7, 9, 13, 18-21] and concrete [3-5, 10] safety barriers. The vehicle models used for the tests of this kind are taken from the US National Crash Analysis Center (NCAC) website [27].

In the case of steel safety barriers, analyses are predominantly carried out for straight barriers with various containment levels [6, 7, 15, 21], in compliance with the standards in force [23, 24]. Publication [15] deals with a selected roadside barrier of the N2-W4-A class with a B-type guiderail profile, forming a horizontal concave arc and situated in a horizontal bend of a fast traffic trunk road, for which the road centreline radius should be within limits of 140-220 m. It was shown that the results of the TB11 crash test could not be accepted for the said safety barrier in a configuration as specified above. To bring the barrier to conformity with the requirements for the TB11 crash test results, a composite-foam cover rail, given a code CFR2, was designed, which was attached to the B-type guiderail

profile by means of bolted joints, utilizing only the free holes in the guiderail profile centreline, spaced in 2.00 m intervals. A method of numerical modelling and simulation of the non-modified and modified TB11 crash test was developed, applicable to the straight and curved barrier, respectively, for the barrier with and without the CFR2 cover rail. The virtual crash tests TB11 were carried out for the said four barrier configurations. The Geo Metro vehicle model was taken from the public library of the US National Crash Analysis Center (NCAC) [27] and modified according to the needs. For the crash test simulations, the LS-Dyna v971 system was used. In result of the tests, the barrier with the cover rail, forming a horizontal concave arc, was found to meet the requirements of the TB11 crash tests.

Results of the simulation of crash tests with a light vehicle hitting a barrier in the form of a horizontal arc with a radius of about 12 m, provided with a W-type guiderail profile, have been presented in publication [18]. The vehicle model was taken from the NCAC library [27]. The impact velocity was 40 km/h, 60 km/h, and 80 km/h. In all the cases, the vehicle hit the barrier at an angle close to 0 ° and slid on it with no major damage. Finally, the vehicle-barrier interaction was terminated in a correct way. The objective of the tests was to compare the values of the Acceleration Severity Index (ASI). The effects of an impact of the Geo Metro vehicle against a concrete safety barrier forming a horizontal arc with a radius of 50 m, 100 m, and 200 m as well as the effects of the direction of the pre-impact vehicle motion have been analysed in publication [3].

Modifications to a road barrier of the H1 containment level, based on results of virtual crash tests TB11 and TB42, have been presented in publications [6] and [7], where the authors examined the impact of four design changes: 1) introduction of a tension belt, 2) introduction of a roller guide system, 3) introduction of a rope in the top part of the guiderail profile, 4) introduction of a rope in the bottom part of the guiderail profile.

2. System under test and crash tests covered by the scope of the analysis

This article is dedicated to the SP-05/2 barrier of the N2-W4-A class, manufactured by Stalprodukt S.A., seated in Bochnia, Poland [26]. This barrier system may be used in both the roadside and median barriers (the latter comprising two symmetrical parallel guiderails). The barrier consists of B-type guiderail profile segments of 4.30 m total length each (the effective length is 4.00 m), Sigma posts 1.9 m long, trapezoidal brackets, and rectangular washers. All the barrier components are made of structural steel S235JR. Individual system components are subjected to the hot-dip galvanizing process. As the fasteners, M16 bolts of the 4.6 class with nuts are used [25, 26].

The acceptance requirements for vehicle restraint (barrier) systems of the N2 containment level are specified in the PN-EN 1317 standards [23, 24] in the form of certain criteria that are to be met in the TB11 and TB32 crash tests (in the TB11 procedure, a passenger car with a mass of 900 kg hits the barrier under test with a velocity of 100 km/h at an incidence angle of 20 °; in the TB32 procedure, the mass of the passenger car used as the test vehicle is to be 1 500 kg and its velocity is to be 110 km/h, with the incidence angle being 20 ° again). The approval crash tests of the vehicle restraint systems are carried

out on straight barrier sections. In the works described in [15, 17, 20], the SP-05/2 system in the form of a horizontal concave arc with a radius of 150 m was found to fail the barrier acceptance criteria as specified in the standards in force [23, 24], based on the TB11 and TB32 virtual crash tests. The radius of 150 m is the smallest curvature radius of the outer barriers in bends of the roads classified in Poland under the GP code. For the curved road barriers of the SP-05/2 system to be brought to conformity with the acceptance criteria, a composite-foam cover rail CFR2 was designed [15, 16, 20].

The CFR2 cover rail consists of polyester-glass composite segments partly filled with polyurethane foam (Figs. 1 and 2 [15]). Each segment is 4.70 m long in total, with its effective length being 4.00 m (Figs. 1 and 3 [15]). The cross-section of the CFR2 cover rail has been designed to fit the B-type guiderail profile of the barrier. The composite shells of the CFR2 cover rail profile are made of Polimal P-104TS resin, used as the matrix material and manufactured by Organika-Sarzyna of Sarzyna, Poland; glass mat E, type EM450, and glass fibre fabric E, type STR600, used as the reinforcement material and manufactured by Krosglass of Krosno, Poland; as well as isophthalic gelcoat and topcoat made flame-retardant, in the RAL 7035 colour, used as protective layers. Individual layers of the front composite shell 4 mm thick are laid in the following sequence: gelcoat, glass mat EM450, and two layers of glass fibre fabric STR600. The consecutive layers of the back composite shell 1.5 mm thick are glass mat EM450 and topcoat. The trapezoidal channels formed by the composite shells are filled with polyurethane foam PUR S 42 of 42 kg/m³ mass density, over a length of 3.90 m.

The CFR2 cover rail is fastened to the B-type guiderail profile with bolts M15×80 of class 8.8 with nuts, rectangular EPDM 70°ShA rubber pads, and A-type rectangular steel washers, as specified in the product catalogue published by Stalprodukt S.A., with utilizing the blank holes in the B-type guiderail profile of the SP-05/2 system (Fig. 3). A complete description of the CFR2 cover rail is available from publications [15, 16, 20].

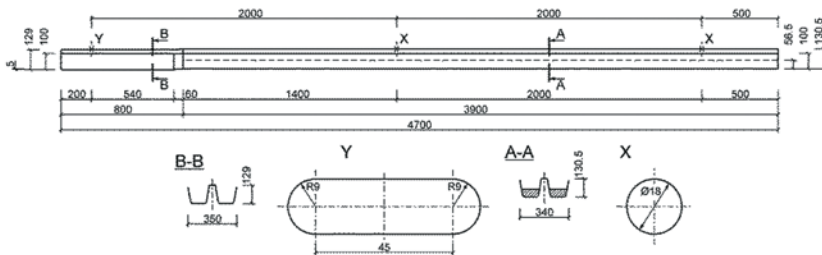


Fig. 1. Segment of the CFR2 cover rail

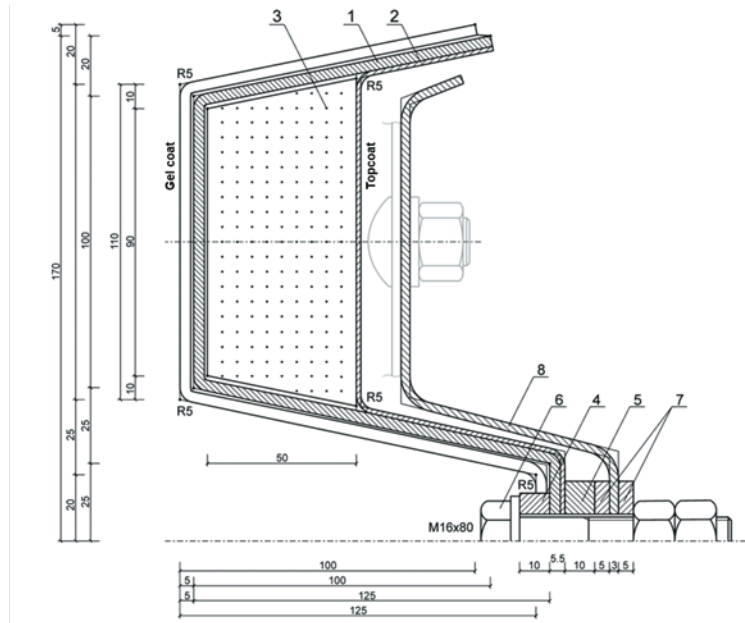


Fig. 2. Cross-section of the CFR2 cover rail at the centreline of the X joint: 1 – front composite shell; 2 – back composite shell; 3 – polyurethane foam; 4 – front rubber pad; 5 – back rubber pad; 6 – steel bolt; 7 – A-type rectangular washer; 7 – B type guiderail profile [15]

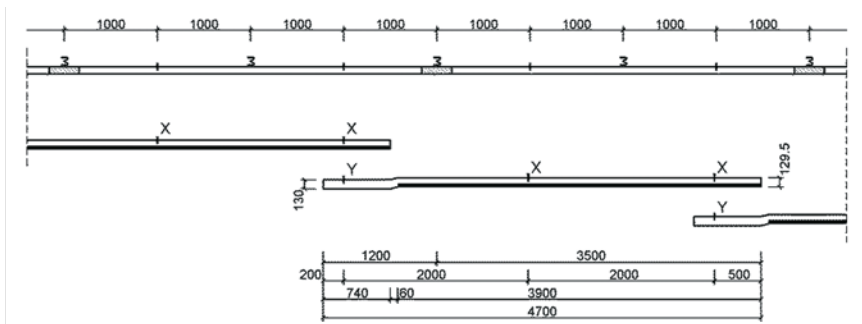


Fig. 3. Schematic diagram of the installation of the CFR2 cover rail on the B type guiderail profile of the SP-05/2 system

3. Numerical models of the systems under analysis

In the modified TB11 virtual crash tests under analysis (with a barrier forming a horizontal concave arc with a radius of 150 m), the Geo Metro vehicle model developed by NCAC [27] was used. The model comprises over 33 000 finite elements. The preliminary virtual crash tests, which included simulations of a central impact of a vehicle against a rigid wall and an impact of the vehicle against the wall at an angle of 20 °, revealed the necessity of introducing a number of modifications and supplements to the model, such as a change in the tyre operation model, correction to the suspension model, introduction of dynamic relaxation (due to gravitation) preceding the start of the process of vehicle collision with the barrier, as well as corrections to the contact options of the model and to the control cards [15].

A test section of the SP-05/2 barrier in the form of an arc with a radius of 150 m, 60 m long, was meshed with 4-node finite shell elements in the Belytschko-Tsay formulation, with reduced integration in the element plane (ELFORM_2 formulation according to [11, 12]). The steel SIGMA posts of the SP-05/2 barrier, embedded in soil, were represented with cylinders 1.30 m high, with a radius of 1.00 m, meshed with solid elements of the HEX8 and PENTAG topology, with the ELFORM_1 formulation assigned to them (solid elements with constant integration) [11, 12]. The composite components of the CFR2 cover rail were meshed with finite elements identical to those used for the steel components of the SP-05/2 barrier (QUAD4 topology, ELFORM_2 formulation), with declaring one integration point per each composite shell layer [11, 12]. The polyurethane foam was represented with a system of 8-node solid finite elements with the ELFORM_1 formulation.

A substantial impact on the functionality of the safety barriers is exerted by the screw fasteners. It is very important that their stiffness and failure should be correctly represented. The bolted joints between guiderail profile segments were represented with beam elements having appropriate stiffness characteristics (according to material model *MAT_68: *MAT_NONLINEAR_PLASTIC_DISCRETE_BEAM [11, 12]). These data were obtained from 3D modelling of the bolted joints [14, 20]. The bolted joints between the CFR2 cover rail and the SP-05/2 barrier system and between the SIGMA posts and the B type guiderail profile segments were modelled with using the *CONSTRAINED_GENERALIZED_WELD_SPOT option, with taking into account appropriate load capacity values according to specific bolt strength class [2].

There are several different materials in the modified SP-05/2 barrier system. They were represented with various material models available in the LS-Dyna system [11, 12]. The components made of steel S235JR (as specified for the SP-05/2 system) were represented with elastic-plastic model *MAT_024: *MAT_PIECEWISE_LINEAR_PLASTICITY with isotropic hardening, with taking into account a failure criterion based on effective plastic strains. The material constants were taken from the product quality certificate issued by Stalprodukt S.A. The polyester-glass composite shells incorporated in the CFR2 cover rail were represented with linear-elastic-brittle material model *MAT_054: *MAT_ENHANCED_COMPOSITE_DAMAGE, with the Chang-Chang failure criterion being taken into account. This model is chiefly used for representing the unidirectionally reinforced composites and woven fabrics, as shown in publication [22]. The elasticity and strength constants of laminas of the composite material of the cover rail were determined from experimental identification tests carried out at the Laboratory of Strength of Materials and Constructions, Department

of Mechanics and Applied Computer Science, Faculty of Mechanical Engineering, Military University of Technology [20]. The polyurethane foam was represented with material model *MAT_026: *MAT_HONEYCOMB. The material constants for the PUR S 42 polyurethane foam were taken from publication [8]. The soil in which the steel SIGMA posts of the SP-05/2 barrier system were embedded was represented with material model *MAT_005: *MAT_SOIL_AND_FOAM. This is a simple model used to represent the behaviour of foams and soils in the case when not all of their material constants are available. The material constants of the soil were taken from the NCAC website [27].

4. Modified TB11 virtual crash tests of the SP-05/2 barrier system, taken as a base

The SP-05/2 barrier system of the N2-W4-A class meets the current standard requirements [23, 24] for the straight barrier section, according to the product catalogue published by Stalprodukt S.A. The results of the TB11 and TB32 virtual crash tests of the SP 05/2 system, as presented in publications [15, 17, 20], were consistent with the experimental crash test results quoted in publication [26]. The TB11 virtual crash tests carried out for the barrier forming a horizontal concave arc with a radius of 150 m, in versions without a cover rail (code TB11/CB/20) and with the CFR2 cover rail (code TB11/CBC/20) have been named "base virtual crash tests". Results of the simulated base crash tests have been presented in Figs. 4 and 5. In the TB11/CB/20 test, the vehicle sideslipped, which is unacceptable according to the relevant standards [23, 24]. This means that the SP 05/2 system in the form of an arc with a radius of 150 m has failed in the crash test required. Thanks to the introduction of the CFR2 cover rail to the system under analysis (Fig. 5), the test vehicle was correctly driven out from its interaction with the barrier.

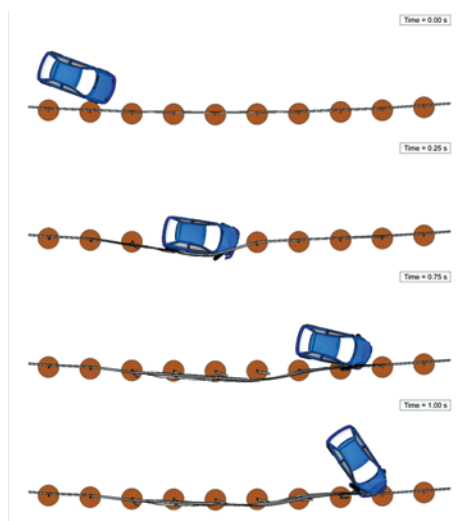


Fig. 4. Animation of the TB11/CB/20 crash test: top view [15]

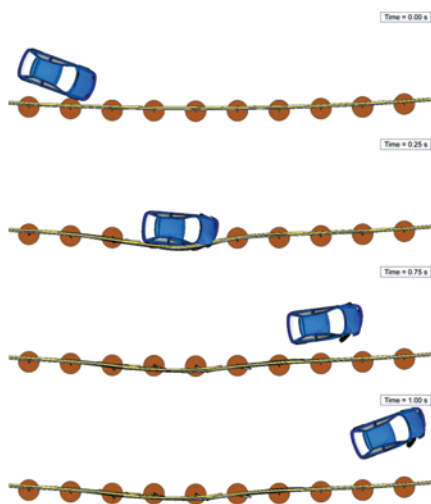


Fig. 5. Animation of the TB11/CBC/20 crash test: top view [15]

A comparison between energy balances in the above crash tests has been shown in Fig. 6. In the TB11/CB/20 crash test, 95 % of vehicle's kinetic energy was absorbed in result of the collision; the energy absorbed due to material damage totalled 0.195 MJ. In the TB11/CBC/20 crash test, 79 % of vehicle's kinetic energy was absorbed in result of the collision and the energy absorbed due to material damage totalled 0.161 MJ. The residual vehicle's velocity at the end of the vehicle-barrier interaction was 47.5 km/h.

Results of the base TB11/CB/20 and TB11/CBC/20 virtual crash tests have been given in Table 2. The CFR2 cover rail was found to have a significant influence on the course of the TB11 crash test carried out on the curved barrier, chiefly thanks to the fact that the SP 05/2 system with the CFR2 cover rail correctly drove the vehicle out from its interaction with the barrier. In the TB11/CBC/20 test compared with the TB11/CB/20 test, the ASI (Acceleration Severity Index) value declined by 5.9 %, the THIV (Theoretical Head Impact Velocity) value was reduced by 8.1 %, the working width (W) decreased by 15.3 %, and the vehicle-barrier interaction length (L) was shortened by 47.2 %.

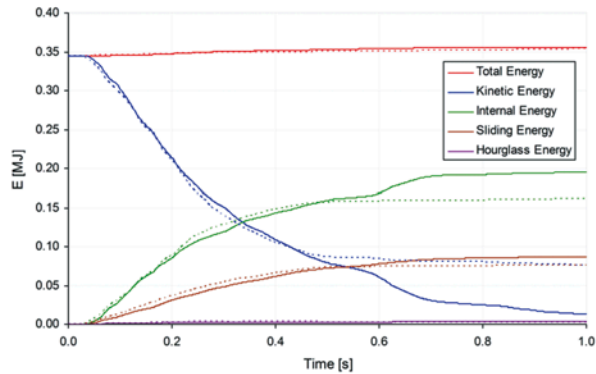


Fig. 6. Comparison of energy balances of the TB11/CB/20 (solid lines) and TB11/CBC/20 (dotted lines) virtual crash tests

5. CFR2 cover rail design parameters under analysis

To show that the design of the CFR2 cover rail was correct and sufficient for the obtaining of satisfactory results of the TB11 virtual crash tests on a barrier forming a horizontal concave arc with a radius of 150 m, the influence of selected design parameters of the cover rail on the barrier performance was examined by carrying out a series of numerical tests. The crash tests covered by the numerical analysis have been listed in Table 1.

Table 1. Crash tests covered by the numerical analysis of the influence of selected parameters on the barrier performance

Test and system code	System modification	Objective of the numerical tests
TB11/CBC/20_NF	Cover rail made without the foam fill and the back composite shell	To determine the influence of the foam fill and the back composite shell
TB11/CBC/20_45	Changed configuration of the woven fabrics in the front composite shell [45/-45]	To determine the influence of the sequence of layers in the front composite shell
TB11/CBC/20_1 TB11/CBC/20_2	One or two layers reinforced with woven fabric (in the [0/90] configuration) added to the front composite shell	To determine the influence of the thickness of the front composite shell

6. Influence of the foam fill and the back composite shell

Results of the simulation of the TB11/CBC/20_NF crash test have been presented in Fig. 7. During the collision, one segment of the cover rail was damaged and broken off from the guiderail profile (the bolted joints were destroyed). The vehicle damage and deformation

was limited to the front wheel set. The vehicle sideslipped within the standard Exit Box, which was unacceptable according to the relevant standards [23, 24].

A comparison between energy balances in the TB11/CBC/20 and TB11/CBC/20_NF crash tests has been shown in Fig. 8. In the TB11/CBC/20_NF crash test, 84.9 % of vehicle's kinetic energy was absorbed in result of the collision; the energy absorbed due to material damage totalled 0.180 MJ. The residual vehicle's velocity at the end of the vehicle-barrier interaction was 43.6 km/h. Results of the TB11/CBC/20_NF virtual crash test have been given in Table 2. The foam fill and the back composite shell of the CFR2 cover rail proved to have a crucial influence on the course of the TB11 virtual crash test carried out on the curved barrier. These components ensure the TB11 crash test results to be accepted.

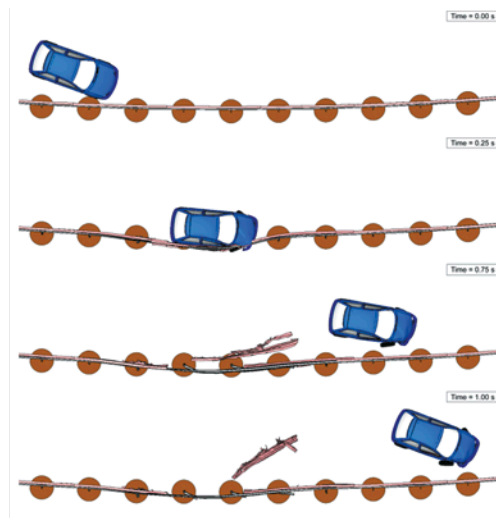


Fig. 7. Animation of the TB11/CBC/20_NF crash test: top view

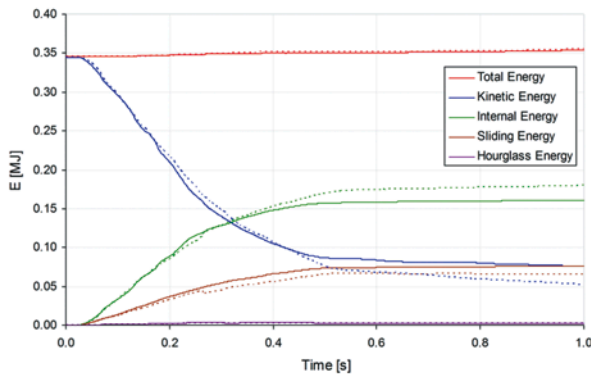


Fig. 8. Comparison of energy balances of the TB11/CBC/20 (solid lines) and TB11/CBC/20_NF (dotted lines) virtual crash tests

7. Influence of the sequence of layers in the front composite shell

Results of the simulation of the TB11/CBC/20_45 crash test have been presented in Fig. 9. The trajectory of the test vehicle was correct. A comparison between energy balances in the TB11/CBC/20 and TB11/CBC/20_45 crash tests has been shown in Fig. 10. In the TB11/CBC/20_45 crash test, 75.6 % of vehicle's kinetic energy was absorbed in result of the collision; the energy absorbed due to material damage totalled 0.211 MJ. The residual vehicle's velocity at the end of the vehicle-barrier interaction was 55.3 km/h.

Results of the TB11/CBC/20_45 virtual crash test have been given in Table 2. In the TB11/CBC/20_45 test compared with the TB11/CBC/20 test, the ASI value declined by 7.5 %, the THIV value was reduced by 12.6 %, the working width (W) decreased by 1.4 %, and the vehicle-barrier interaction length was shortened by 16.2 %. The residual vehicle's velocity at the end of the vehicle-barrier interaction was higher by 16.4 %.

A change in the sequence of the configuration of layers in the front composite shell of the CFR2 cover rail from [0/90] to [45/-45] resulted in an improvement in most of the collision parameters. However, the vehicle's behaviour became close to sideslipping within the standardized Exit Box. Moreover, the CFR2 cover rail with the [45/-45] configuration of layers in the front composite shell is more expensive.

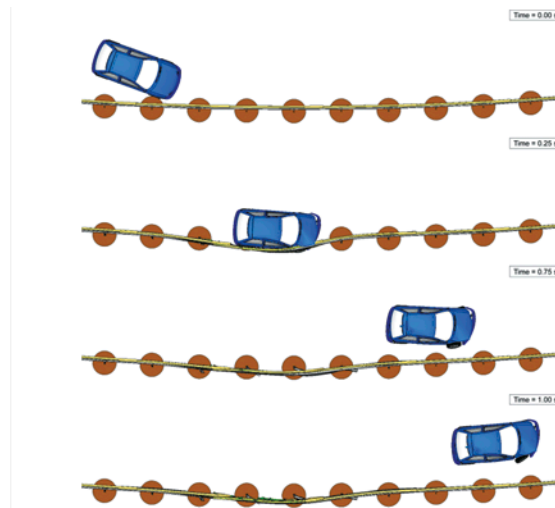


Fig. 9. Animation of the TB11/CBC/20_45 crash test: top view

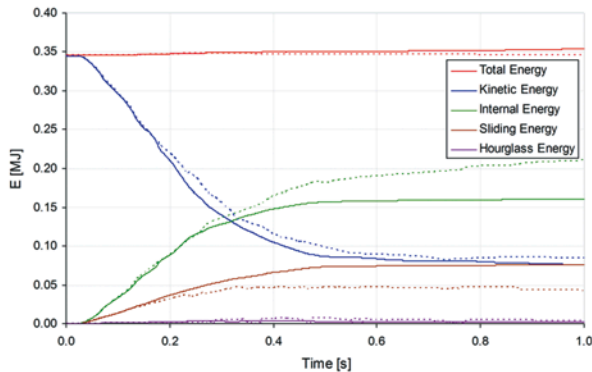


Fig. 10. Comparison of energy balances of the TB11/CBC/20 (solid lines) and TB11/CBC/20_45 (dotted lines) virtual crash tests

8. Influence of the thickness of the front composite shell

Results of the simulation of the TB11/CBC/20_1 and TB11/CBC/20_2 crash tests have been presented in Figs. 11 and 12. A comparison between energy balances in the TB11/CBC/20, TB11/CBC/20_1, and TB11/CBC/20_2 crash tests has been shown in Fig. 13. In the TB11/CBC/20_1 crash test, 65.9 % of vehicle's kinetic energy was absorbed in result of the collision; the energy absorbed due to material damage totalled 0.165 MJ. The residual vehicle's velocity at the end of the vehicle-barrier interaction was 61.0 km/h. The damage to the Geo Metro vehicle was insignificant. In the TB11/CBC/20_2 crash test, 74.2 % of vehicle's kinetic energy was absorbed in result of the collision and the energy absorbed due to material damage totalled 0.143 MJ. The residual vehicle's velocity at the end of the vehicle-barrier interaction was 57.3 km/h. The damage to the Geo Metro vehicle was insignificant, too.

Results of the TB11/CBC/20_1 and TB11/CBC/20_2 virtual crash tests have been given in Table 2. In the TB11/CBC/20_1 test compared with the TB11/CBC/20 test, the THIV value was reduced by 11.7 %, the working width decreased by 5.6 %, and the vehicle-barrier interaction length was shortened by 15.4 %. The residual vehicle's velocity at the end of the vehicle-barrier interaction was higher by 28.4 %. The ASI value was identical. In the TB11/CBC/20_2 test compared with the TB11/CBC/20 test, the ASI value declined by 8.8 %, the THIV value was reduced by 10.8 %, the working width decreased by 8.3 %, and the vehicle-barrier interaction length was shortened by 15.4 %. The residual vehicle's velocity at the end of the vehicle-barrier interaction was higher by 20.6 %.

The adding of a single layer of woven fabric in the [0/90] configuration to the front composite shell of the CFR2 cover rail resulted in an improvement in some of the collision parameters, (e.g. THIV, \bar{W} , v_r). However, the cover rail without an additional reinforcement layer, i.e. less expensive, was sufficient for the obtaining of very good collision parameters and for

the barrier to pass the TB11 crash test. The adding of one more layer of the [0/90] woven fabric (i.e. the applying of two additional layers in total) did not considerably improve the collision parameters.

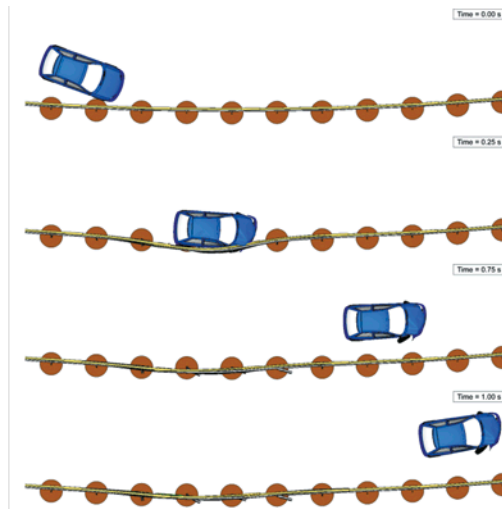


Fig. 11. Animation of the TB11/CBC/20_1 crash test: top view

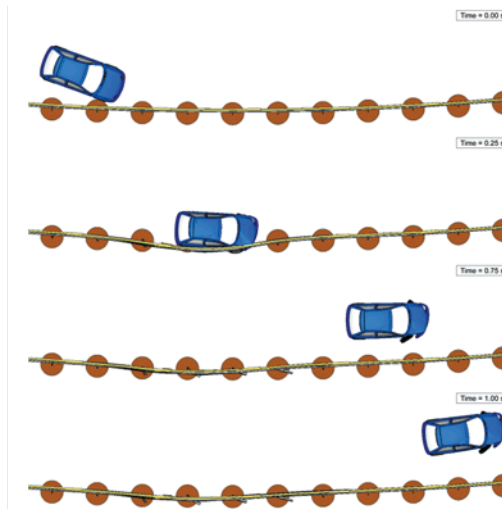


Fig. 12. Animation of the TB11/CBC/20_2 crash test: top view

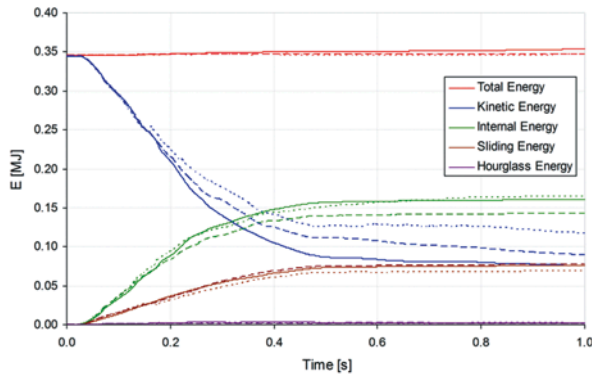


Fig. 13. Comparison of energy balances of the TB11/CBC/20 (solid lines), TB11/CBC/20_1 (dashed lines) and TB11/CBC/20_2 (dotted lines) virtual crash tests

Table 2. Comparison of results of the virtual crash tests

Dynamic system (Test code)	ASI	THIV [km/h]	VCDI ¹⁾	W [m]	$L^{2)}$ [m]	PPO ³⁾	$E^{4)}$ [MJ]	$v_r^{5)}$ [km/h]
TB11/CB/20	0.85	20.91	RF0010000	0.85	12.3	No	0.195	–
TB11/CBC/20	0.80	19.21	RF0010110	0.72	6.50	Yes	0.161	47.5
TB11/CBC/20_NF	1.01	16.12	RF0011000	0.68	5.85	No	0.180	43.6
TB11/CBC/20_45	0.74	16.78	RF0000000	0.71	5.45	Yes	0.211	55.3
TB11/CBC/20_1	0.80	16.96	RF0010000	0.68	5.50	Yes	0.165	61.0
TB11/CBC/20_2	0.73	17.13	RF0010000	0.66	5.50	Yes	0.143	57.3

¹⁾ Vehicle Cockpit Deformation Index

²⁾ Vehicle-barrier integration length

³⁾ Correct vehicle's behaviour in the Exit Box

⁴⁾ Energy absorbed due to material damage

⁵⁾ Residual velocity

9. Recapitulation

The paper presents the influence of selected design parameters of a CFR2 composite-foam cover rail on the course of the TB11 virtual crash test carried out on an SP-05/2 barrier forming a horizontal concave arc with a radius of 150 m. The cover rail design parameters subject to modification whose impact was examined included the application of the foam fill and the back composite shell as well as the sequence of reinforcement layers in the front composite shell and the thickness of this shell.

The following conclusions may be drawn from the TB11 virtual crash tests carried out.

- 1) The foam fill and the back composite shell are very important components of the CFR2 cover rail. Without these elements, the said cover rail loses its functionality. In the TB11 virtual crash test carried out on the SP-05/2 barrier forming a horizontal concave arc with a radius of 150 m, one of the cover rail segments broke off from the vehicle restraint system and a sideslip of the test vehicle took place.
- 2) A change in the sequence of configuration of the reinforcement fabric layers in the front composite shell of the CFR2 cover rail from [0/90] to [45/-45] resulted in an improvement in most of the collision parameters. However, the behaviour of the test vehicle being redirected to the carriageway was worse, as the vehicle was close to sideslipping.
- 3) The adding of one or more layers of the [0/90] woven fabric to the front composite shell in the CFR2 cover rail structure did not considerably improve the collision parameters. The cover rail without an additional reinforcement layer, i.e. less expensive, was sufficient for the obtaining of very good collision parameters and for the barrier to pass the TB11 crash test.

The numerical analyses carried out showed the design of the CFR2 cover rail as proposed in [15] to be correct and sufficient for the TB11 crash test results to be accepted.

Acknowledgements

This work was done within research project No. PBS1/B6/14/2012 (acronym: ENERBAR), sponsored by the National Centre for Research and Development, Poland, in 2013-2015.

The full text of the article is available in Polish online on the website <http://archiwummotoryzacji.pl>

Tekst artykułu w polskiej wersji językowej dostępny jest na stronie <http://archiwummotoryzacji.pl>

References

- [1] Atahan A O. Finite element simulation of a strong-post W-beam guardrail system. *Simulation*. 2002; 10 (78); 587-599.
- [2] Biegus A. Połączenia śrubowe (Bolted joints). Wydawnictwo Naukowe PWN. Warszawa-Wrocław 1997.
- [3] Borkowski W, Hryciów Z, Rybak P, Wysocki J. Analiza skuteczności betonowych barier ochronnych na łuku drogi (Analysis of the effectiveness of concrete protective barriers on the road curve). *Przegląd Mechaniczny*. 2012 (LXXI); 7-8; 21-24.
- [4] Borkowski W, Hryciów Z, Rybak P, Wysocki J. Numerical simulation of the standard TB11 and TB32 tests for a concrete safety barrier. *Journal of KONES Powertrain and Transport*. 2010 (17); 4; 63-71.
- [5] Borkowski W, Hryciów Z, Rybak P, Wysocki J. Testing the results of a passenger vehicle collision with a rigid barrier. *Journal of KONES Powertrain and Transport*. 2010 (17); 1; 51-57.

- [6] Borovinsek M, Vesenjok M, Ulbin M, Ren Z. Simulating the impact of truck on road-safety barrier. *Journal of Mechanical Engineering*. 2006 (52); 2; 101-111.
- [7] Borovinsek M, Vesenjok M, Ulbin M, Ren Z. Simulation of crash test for high containment levels of road safety barriers. *Engineering Failure Analysis*. 2007 (14); 1711-1718.
- [8] Dziewulski P. Examination of Selected Structures to Improve Energy Intensity of Road Safety Barriers (in Polish). PhD Thesis, Military University of Technology, Warsaw, Poland. 2010.
- [9] Dziewulski P. Numerical analysis of car-road barrier crash tests [in Polish]. *Proceedings of the 3rd Symposium on Advances in Manufacturing Technologies and Machinery Structures*. Kazimierz Dolny, Poland. 2009; 43-49.
- [10] Goubel C, Di Pasquale E, Massenzio M, Ronel S. Comparison of crash tests and simulations for various vehicle restraint systems. 7th European LS-DYNA Conference. DYNAmore GmbH. 2009; CD Proceedings; 1-12.
- [11] Hallquist J O. LS-DYNA Keyword User's Manual. Livermore Software Technology Corporation. Livermore, CA, USA. May 2007.
- [12] Hallquist J O. LS-DYNA Theory Manual. Livermore Software Technology Corporation. Livermore, CA, USA. March 2006.
- [13] Kiczko A, Niezgoda T, Nowak J, Dziewulski P. Numerical implementation of car impact into the modified road barrier. *Journal of KONES Powertrain and Transport*. 2010 (17); 3; 189-196.
- [14] Klasztorny M, Kiczko A, Nycz D. Modelowanie numeryczne i symulacja rozciągania połączenia śrubowego segmentów prowadnicy B bariery drogowej (Numerical modelling and simulation of tension in the bolted joint of the B-type guiderail of a road barrier). 13th Scientific and Technical Conference "Computer Techniques in Engineering". Licheń Stary. 2014; 77-78.
- [15] Klasztorny M, Nycz D B, Romanowski R K. Rubber/foam/composite overlay onto guide B of barrier located on road bend. *The Archives of Automotive Engineering*. 2015; 3 (69); 65-86.
- [16] Klasztorny M, Romanowski R K, Nycz D B. Nakładka kompozytowo-pianowa na prowadnicę B drogowej bariery ochronnej w łuku poziomym wklęsłym. Część 1: Projekt nakładki na prowadnicę bariery SP-05/2 (Composite-foam cover rail for the B-type guiderail of a road safety barrier formed into a horizontal concave arc. Part 1: Engineering design of a cover rail for the guiderail of the SP-05/2 barrier). *Materiały kompozytowe*. 2015; 3; 36-38.
- [17] Klasztorny M, Romanowski R K, Nycz D B. Nakładka kompozytowo-pianowa na prowadnicę B drogowej bariery ochronnej w łuku poziomym wklęsłym. Część 2: Modelowanie i symulacja testów zderzeniowych (Composite-foam cover rail for the B-type guiderail of a road safety barrier formed into a horizontal concave arc. Part 2: Modelling and simulation of crash tests). *Materiały kompozytowe*. 2015; 4; 8-10.
- [18] Nasution R P, Siregar R A, Fuad K, Adom A H. The effect of ASI (Acceleration Severity Index) to different crash velocities. *International Conference on Applications and Design in Mechanical Engineering (ICADME)*. Malaysia. 11-13 October 2009; CD Proceedings; 1-6.
- [19] Niezgoda T, Barnat W, Dziewulski P, Kiczko A. Numerical modelling and simulation of road crash tests with the use of advanced CAD/CAE systems. *Journal of KONBIN*. 2012; 3 (23); 95-108.
- [20] Nycz D. Modelowanie i badania numeryczne testów zderzeniowych bariery klasy N2-W4-A na łukach dróg (Modelling and numerical examination of crash tests for barriers of the N2-W4-A class in road bends). Wydawnictwo WAT (Publishing House of the Military University of Technology). Warszawa 2015.
- [21] Vesenjok M, Borovinsek M, Ren Z. Computational simulations of road safety barriers using LS-DYNA. 6. LS-DYNA Anwenderforum. DYNAmore GmbH, Frankenthal. 2007; CD Proceedings; 1-8.
- [22] Wade B, Feraboli P, Osborne M. Simulating laminated composites using LS-DYNA material model MAT54 part I: [0] and [90] playsingle-element investigation [cited: 2014 Sep 22]. Available from: https://depts.washington.edu/amtas/events/jams_12/papers/paper-feraboli.pdf.
- [23] PN-EN 1317-1:2010. Systemy ograniczające drogę – część 1: Terminologia i ogólne kryteria metod badań (Road Restraint Systems. Part 1: Terminology and general criteria for test methods).
- [24] PN-EN 1317-2:2010. Systemy ograniczające drogę – część 2: Klasy działania, kryteria przyjęcia badań zderzeniowych i metody badań barier ochronnych i balustrad (Road Restraint Systems. Part 2: Performance classes, impact test acceptance criteria and test methods for safety barriers including vehicle parapets).
- [25] Stalowe bariery ochronne (Steel safety barriers). Stalprodukt S.A. Bochnia, Poland. 2006.
- [26] System N2 W4 (SP-05/2). Stalprodukt S.A. Bochnia, Poland. 2011.
- [27] <http://www.ncac.gwu.edu/vml/models.html>, Vehicle Models, NCAC, USA, January 7, 2013.